

Sagittarius, a dwarf spheroidal galaxy without dark matter?

M.A. Gómez-Flechoso, R. Fux and L. Martinet

Geneva Observatory, Ch. des Maillettes 51, CH-1290 Sauverny, Switzerland

Received / Accepted

Abstract. The existence of dwarf spheroidal galaxies with high internal velocity dispersions orbiting in the Milky Way raises questions about their dark matter content and lifetime. In this paper, we present an alternative solution to the dark matter dominated satellites proposed by Ibata & Lewis (1998) for the Sagittarius dwarf galaxy. We performed simulations of two kinds of N-body satellites: the first models (f-models) could correspond to satellites with high dark matter content and they represent initially isolated models. The second models (s-models) have either low or negligible dark matter content and they are constructed in a tidal field. In spite of being on the same orbits, the s-models are able to produce a better agreement with some observational constraints concerning Sagittarius. From our simulations, we can also infer that Sagittarius is in the process of being disrupted.

Key words: Galaxies: local group, interactions. Methods: numerical

1. Introduction

The current interest for dwarf spheroidal galaxies (hereafter DSphs) as satellites of the Milky Way is raised by two fundamental questions concerning their evolution: the real content of dark matter (DM) in these objects (see, for example, Mateo 1994,1997,1998; Piatek & Pryor 1995; Burkert 1997 and references therein) and their implication in the hierarchical formation of the galactic halo (e.g., Johnston et al. 1996).

The Sagittarius (Sgr) dwarf galaxy is the closest known satellite galaxy to the center of the Milky Way, $R_{GC} \sim 16$ kpc (Ibata et al. 1995, 1997). Due to its proximity we can expect from its study an additional contribution to our understanding of DSphs in general. Since the announcement of its discovery by Ibata et al. (1994) the structure and evolution of Sgr have been extensively discussed and simulated by various authors: Ibata et al. (1995), Johnston et al. (1995), Velázquez & White (1995), Whitelock et al. (1996), Mateo et al. (1996), Alard (1996), Ibata et al. (1997), Edelson & Elmegreen (1997), Layden & Saragadini (1997), Ibata & Lewis (1998), Mateo et al. (1998). Important problems concerning this system are: 1) its possible lifetime before dissolution, 2) the possible presence of

Table 1. Observational parameters of Sagittarius dwarf galaxy (Ibata et al. 1997)

| Parameter | |
|---------------|-------------------------------|
| r_{hb} | 0.55 kpc |
| σ_o | 11.4 km/s |
| μ_{oV} | 25.4 mag/arcsec ² |
| L_t | $\geq 10^7 L_\odot$ |
| $(M/L)_o$ | $50 M_\odot/L_\odot$ |
| M_t | $> 10^9 M_\odot$ |
| $(l, b)^a$ | (5.6°, -14°) |
| $(U, V, W)^b$ | (232,0,194)± 60 km/s |
| d_\odot^c | 25 kpc |
| R_{GC}^d | 16 kpc |
| v_r^e | 171 km s ⁻¹ |
| $(dv/db)^f$ | -3 km s ⁻¹ /degree |

^a Galactic coordinates

^b Galactic velocities

^c Heliocentric distance

^d Galactocentric distance

^e Radial velocity

^f Gradient of the radial velocity

DM in it. A critical point in the studies mentioned above is the question whether Sgr is in virial equilibrium or not.

Usually, the total inferred mass of the DSph is calculated by assuming it is in virial equilibrium¹. In this case, the central mass-to-light ratio depends on the velocity dispersion through the equation (Richstone & Tremaine 1986)

$$\left(\frac{M}{L}\right)_o = \eta \frac{9\sigma_o^2}{2\pi G \mu_o r_{hb}} \quad (1)$$

where η is near unity for a wide variety of models, σ_o the central velocity dispersion, μ_o the central surface brightness and r_{hb} the half-brightness radius. The analysis of the validity of Eq. (1) for evolving DSphs has been studied in detail in the present context by Kroupa (1997, hereafter K97).

In Table 1, we have summarized the parameters of Sgr DSph measured by Ibata et al. (1997). For the values of σ_o ,

¹ In this paper, the *inferred mass* is always obtained by assuming a virial equilibrium for the satellite.

r_{hb} and μ_{oV} given in Table 1, those authors obtain a high central mass-to-luminosity ratio $(M/L)_o = 50 M_\odot/L_\odot$ by using the Eq. (1). Therefore, the total inferred mass assuming virial equilibrium, M_t , is DM dominated. The values of total luminosity, L_t , and the total inferred mass, M_t , are also listed in Table 1. However, the values of $(M/L)_o$ and L_t suggested by Mateo et al. (1998) are different. These authors have discovered a tidal extension of Sgr, which implies $L_t \leq 5.8 \times 10^7 L_\odot$ and, as a consequence, the $(M/L)_o$ ratio could decrease to $10 M_\odot/L_\odot$. Adopting the structural and orbital characteristics usually assumed (given in Table 1), Ibata et al. (1997) recently suggested that such a satellite galaxy is expected to be tidally disrupted and destroyed after several pericentric passages, unless a significant quantity of DM is present inside it, as inferred assuming virial equilibrium. The observations of the Sgr globular clusters give an age spread of its constituents > 4 Gyrs and the youngest globular cluster (Terzan 7) is 9-13 Gyrs old (Montegriffo et al. 1998). The fast disruption obtained by the numerical methods raise the question about the age and the dynamical history of Sgr. However, it must be emphasized that the initial time $t = 0$ of the simulations does not necessarily coincide with the time of formation of the oldest constituents of the satellite.

The partial formation of the galactic halo by hierarchical processes (accretion of small galaxies) has recently received an increase of interest, stimulated for instance by the investigation by Lynden-Bell & Lynden-Bell (1995) on the reality of streams (Lynden-Bell 1982) in the close environment of the Milky Way, among them the well known Magellanic Stream. DSphs seem to belong to one or another of these streams and their evolution clearly depends on their environment. This scenario of satellite formation involves a low DM content for the DSphs (Barnes & Hernquist 1992; Kroupa 1998). However, the only simulations of no-dark matter satellite galaxies able to survive in a tidal field are those of K97 and Klessen & Kroupa (1998, hereafter KK98). These authors have studied a region in the parameter space (M_{sat}, r_{sat}) , where M_{sat} and r_{sat} are the mass and a typical radius of the satellite, and they have obtained a residual satellite from a more massive one. Nevertheless, their remnant satellite galaxies are fainter than a typical DSph, unless the true $(M/L)_{real} < 3$.

These circumstances make questionable the maintenance of dynamical equilibrium and consequently the virial estimation of mass for these systems.

In this paper we present self-consistent N-body simulations of Sgr and a more accurate and plausible scenario of its evolution, which suggests that Sgr is likely to be able to survive for a long time (6 – 10 Gyr) by orbiting in the Galaxy without being dominated by DM.

In Sect. 2, we present the model of the Milky Way used in our simulations. In Sect. 3, we describe the different models of the satellite galaxy and corresponding scenarios of interaction with the Galaxy. In Sect. 4 some numerical considerations are given. In Sect. 5, we present the results of our simulations for the different chosen scenarios. These results are discussed in Sect. 6 in connection with recent conjectures by

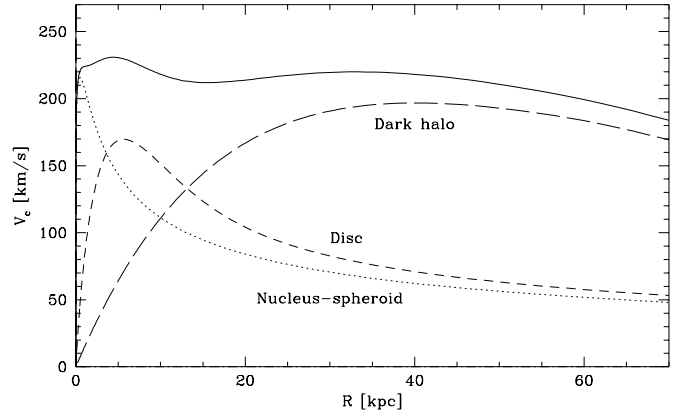


Fig. 1. Rotation curve of the initial Milky Way model (full line), with the contributions of each component

Kroupa (1998b, hereafter K98) on the parameter space possible for progenitors of surviving DSphs without DM. Finally, a summary is given in Sect. 7.

2. The model of the Milky Way

The initial model of the primary galaxy, representing the Milky Way, is based on the axisymmetric initial conditions adopted by Fux (1997) in his N-body modeling of the Galaxy. The mass distribution is divided in three components: (i) an oblate stellar nucleus-spheroid with a spatial density $\rho \propto r^{-1.8}$ in the central region, in agreement with the near-infrared observations of the inner bulge (Becklin & Neugebauer 1968; Matsumoto et al. 1982), and $\propto r^{-3.3}$ outside the bulge, as the number density counts of stellar halo objects (e.g. Preston et al. 1991 for RR Lyrae; Zinn 1985 for globular clusters), (ii) a double exponential stellar disc, with radial and vertical scale lengths $h_R = 2.5$ kpc and $h_z = 250$ pc and (iii) an oblate dark halo with an exponential profile ensuring a roughly flat rotation curve out to $R = 40$ kpc. Both oblate components have a flattening $c/a = 0.5$. The total mass of the luminous component is $M_L = 8.25 \times 10^{10} M_\odot$. The model is identical to Fux’s model m04t0000, except that the dark halo is more extended, with a scale length $b = 13$ kpc and a total (untruncated) mass $M_{DH} = 2.4 \times 10^{11} M_\odot$, and that the truncation radius is moved further away at $R_c = 70$ kpc. The chosen truncation radius ensures a non-vanishing density everywhere along the orbit of the satellite galaxy. The resulting rotation curve of the model is shown in Fig. 1.

The initial kinematics is obtained by solving the hydrodynamical Jeans equations, assuming an isotropic velocity dispersion for the disc component and an anisotropic but centrally oriented velocity ellipsoid for the other components. The velocity distribution of the nucleus-spheroid and dark halo is generated from a 3D generalization of the Beta distribution which limits the number of escaped particles and thus greatly improves the equilibrium of the isolated dynamical model. More details are given in Fux (1997).

3. Satellite models

The effects that a DSph suffers when it is accreted on a primary galaxy strongly depend on its structure and its orbit.

We have considered two kinds of satellite models. They correspond to two scenarios of interaction between the Galaxy and the satellite.

In the first models (f-models), we represent the satellite as a *standard* King’s sphere (King 1966), which matches the observational constraints for the total virial mass, M_t , the core radius, r_o , and the central velocity dispersion, σ_o , of the Sgr DSph. In this case, the effects on the DSph are maximal because the satellite, originally in an isolated situation, suddenly undergoes strong tidal perturbations.

Our alternative scenario (s-models) assumes that either the DSph is formed in the tidal tail of another major accretion event and therefore it is built in equilibrium with the environment, or the DSph falls slowly from a quasi-isolated situation to a tidal field region and it has enough time to readjust itself to the environmental forces. In both situations, we begin our simulations when the satellite has already reached the equilibrium with the dense environment and, therefore, the life time of the DSph orbiting in the galaxy is expected to be longer than in our first scenario. In the present case, the satellite is modelled by a *modified* King’s sphere (Gómez-Flechoso & Domínguez-Tenreiro 1998), which takes into account the tidal potential produced by the primary galaxy.

We have checked several orbits in order to compare the observational features of the Sagittarius dwarf and the numerical results in both fast and slow accreting scenarios. The orbits we have chosen reproduce the present position, (l, b) , and galactocentric velocity, (U, V, W) , of Sagittarius DSph in the observational range (Table 1), and, therefore, the simulated orbits are polar, as suggested by the void component of the proper motion parallel to the Galactic Plane. The orbits are either low eccentricity orbits in the central part of the Galaxy or high eccentricity orbits.

The central mass-to luminosity ratio of the models has been calculated by using the Eq. (1). The central velocity dispersion σ_o involved in this equation has been measured along the line-of-sight. We have removed the particles with the largest radial velocities (relative to the radial velocity of the center of mass of the satellite) to prevent contamination by outlying particles. We have only considered those particles with projected distance to the center of the satellite smaller than 0.5 kpc.

3.1. f-models

The distribution function of an isolated galaxy fulfills the collisionless Boltzmann equation. We can represent an isolated DSph as a solution of this equation. King’s spheres are an example of that.

If an initially isolated DSph reaches the inner regions of a galaxy within a short timescale, it has no time to modify its internal structure. In this case the satellite maintains its isolated King’s sphere distribution function at the beginning of the sim-

Table 2. Physical parameters of the isolated King’s model of Sgr (f-models): core radius, r_o , central velocity dispersion, σ_o , total mass, M_t , dimensionless potential, W_o and tidal radius, r_t

| r_o (kpc) | σ_o (km/s) | M_t ($10^7 M_\odot$) | W_o | r_t (kpc) |
|----------------|----------------------|-----------------------------|-------|----------------|
| 0.527 | 15.0 | 12.0 | 3.26 | 2.736 |

Table 3. Parameters of the orbits of the f-models

| Model | r_{min} (kpc) | r_{max} (kpc) | Period (Gyr) |
|-------|--------------------|--------------------|-----------------|
| f-A | 12 | 18 | 0.23 |
| f-B1 | 8 | 38 | 0.45 |
| f-B2 | 10 | 70 | 0.95 |

ulation. Once in the inner orbit, the satellite will evolve quickly, because tidal forces are strong in these regions. This scenario is unrealistic, because, in reality, a satellite which reaches the denser parts of the galaxy has suffered the influence of the galaxy potential for a long period of time. However, we have run simulations in such a case because they correspond to the common initial conditions assumed in the literature (Johnston et al. 1995, Oh et al. 1995, Velázquez & White 1995, Johnston et al. 1996, Edelsohn & Elmegreen 1997, K97, KK98, Ibata & Lewis 1998) and in order to compare the results with those of the more realistic s-model satellites.

The parameters of the King’s model we have selected for the satellite model in a fast accreting scenario are given in Table 2 and they have been chosen to reproduce the present characteristics of Sagittarius, as was done in other simulations (Velázquez & White 1995). The total mass of the satellite model corresponds to the virial mass inferred for Sgr. Therefore, if the observational constraints on the luminous mass are considered, the satellite model could represent a DM dominated DSph. For these models, we have assumed $(M/L)_{real} = 10 M_\odot/L_\odot$ for the calculations of surface brightness, which is the lower limit of the mass-to-luminosity ratio for DM dominated satellites. A higher $(M/L)_{real}$ would represent fainter satellite galaxies (for the same DM content) and an apparently faster dissolution process.

The initial apocenter and pericenter and the period of the low eccentricity orbit (f-A) and the high eccentricity orbits (f-B1 and f-B2) are listed in Table 3.

3.2. s-models

In the other possible scenario we assume that either the satellite has been formed inside the tidal tail of a major merger (e.g. numerical simulations by Barnes & Hernquist 1992, and the observational counterpart by Duc & Mirabel 1997) or it has been slowly accreted.

In the first case, if the dwarf galaxy is formed in equilibrium with the tidal force of the environment, it does not contain a significant amount of DM (Barnes & Hernquist 1992).

Table 4. Galaxy parameters of the s-model satellites

| Model | r_o (kpc) | σ_o (km/s) | M_t ($10^7 M_\odot$) | W_o | r_t (kpc) |
|-------|----------------|----------------------|-----------------------------|-------|----------------|
| s-A | 0.06 | 11.0 | 0.93 | 3.78 | 0.55 |
| s-B1 | 0.1 | 11.0 | 1.66 | 3.95 | 0.99 |
| s-B2a | 0.1 | 15.0 | 5.27 | 5.42 | 1.93 |
| s-B2b | 0.1 | 11.0 | 2.33 | 4.87 | 1.48 |
| s-B2c | 0.3 | 15.0 | 6.04 | 2.98 | 2.02 |

Table 5. Orbital parameters of the s-model satellites

| Model | r_{min} (kpc) | r_{max} (kpc) | r_{ave} (kpc) | Period (Gyr) |
|-------|--------------------|--------------------|--------------------|-----------------|
| s-A | 15 | 20 | 20 | 0.25 |
| s-B1 | 8 | 40 | 35 | 0.45 |
| s-B2 | 10 | 74 | 50 | 1.25 |

In the second case, according to cosmological models of hierarchical structure formation, satellite systems are produced around massive galaxies. These satellites could contain DM halos (e.g. Cole et al. 1994). Tidal forces could be negligible in the outer regions of the galaxy where the satellite is formed. However, if we assume that the satellite does not go through the denser and central regions of the main galaxy in the first perigalacticon, we could expect that an initially massive satellite falls slowly on the center of the galaxy by dynamical friction, loses part of its mass and reaches a central orbit. In this way, the satellite has time to modify its internal structure and to reach the equilibrium with the environment.

DSphs described in the two last scenarios have to be in equilibrium with the tidal forces of the environment. In the paper by Gómez-Flechoso & Domínguez-Tenreiro (1998), the structural parameters (total mass, M_t , velocity dispersion, σ_o , core radius, r_o , etc.) of a satellite in the tidal field of the primary galaxy have been estimated. Those authors have proved that, in general, a galaxy in a tidal field can be described by a two-parameter distribution function. They have solved altogether the Poisson equation and the collisionless Boltzmann equation for a galaxy, taking into account the potential of the galaxy and the tidal potential of the environment. Only spherical terms of the tidal field were considered in this theory. However, the obtained *equilibrium* solutions are better representations of the system than *isolated* models.

This result suggests that in our problem we could represent a DSph in equilibrium with the tidal field of the primary galaxy as a *modified King's sphere* (see Gómez-Flechoso & Domínguez-Tenreiro 1998) with two free parameters. We have chosen the central velocity dispersion, σ_o , and the core radius, r_o , as input parameters, because both can be determined from observations. In our simulations, the values for these two parameters are $r_o \sim 0.06 - 0.3$ kpc and $\sigma_o \sim 11 - 15$ km/s, which reproduce the characteristics of the Milky Way satellites. Thus, we will try to explain the Sagittarius satellite as a typical

DSph which has evolved orbiting for a long time in the Galaxy potential. The other parameters of the model (total mass, tidal radius and dimensionless central potential) are automatically determined by the tidal potential at each position of the orbit.

The satellite parameters of the models which have been performed are listed in Table 4. The second column is the core radius, r_o , and the third column is the central velocity dispersion, σ_o , which are input parameters of the modified King's spheres. The total mass, M_t , the dimensionless central potential, W_o , and the tidal radius, r_t , (columns 4, 5 and 6) are output parameters obtained by solving the collisionless Boltzmann equation with the tidal potential at the averaged distance of the orbit to the Galaxy center (parameter r_{ave} in Table 5).

As it can be seen in Table 4, the dimensionless central potential and the mass of the satellite decrease for inner positions of the equilibrium satellite for models with the same r_o and σ_o . Furthermore, the mass of the models is smaller than the mass inferred from observations using kinematic arguments (Ibata et al. 1997, Mateo 1994) and it is in agreement with the observed luminous mass, assuming $(M/L)_{real} \sim 2 - 5 M_\odot/L_\odot$. Therefore, we have assumed $(M/L)_{real} = 2 M_\odot/L_\odot$ for all the s-models, that is a typical value for the stellar population of a DSph. The low value of the mass-to-luminosity ratio is in agreement with satellites either formed in tidal tails of major accretion events or tidally modified by orbiting for a long time in a tidal potential.

The apocenter, r_{max} , the pericenter, r_{min} , and the period of the orbits are listed in Table 5. The s-A orbit is an orbit of low eccentricity in the inner region of the Galaxy and s-B1 and s-B2 orbits have higher eccentricity.

4. Numerical details

The models have been evolved using the treecode algorithm kindly provided by Barnes & Hut (1986) with a tolerance parameter $\theta = 0.7$ and a time-step $\Delta t = 1$ Myr. The number of particles of the luminous and dark halo components of the primary galaxy are 15671 and 29648, respectively, and the mass of the dark matter particles is 3 times larger than for the luminous particles. All the satellite models have 4000 equal-mass particles, except s-B2a and s-B2c which have 8000 particles.

We use a softening length varying proportionally to the cubic root of the particle mass of the component, in order to avoid well-known usual numerical effects in the simulations (e.g. Merritt 1996; Theis & Spurzem 1999). For the luminous particles of the Galaxy it is $\epsilon_L = 0.23$ kpc and for the dark matter halo $\epsilon_{DH} = 0.33$ kpc. The f-models have $\epsilon_S = 0.06$ kpc, but this value is changed to $\epsilon_S = 0.05$ kpc for the s-A, s-B1 and s-B2b satellites and $\epsilon_S = 0.04$ kpc for the s-B2a and s-B2c satellites.

5. Results

5.1. The main galaxy

The main galaxy develops a bar-like structure, described by Fux (1997) for an isolated model of our Galaxy.

The global effects of the satellite on the primary galaxy are weak, since the mass ratio of both objects is huge. Besides, the poor resolution of the Galaxy model prevents a detailed description of the local effects of the Sagittarius accretion on the Milky Way. Therefore, we only deal with dynamical effects felt by the satellite galaxy.

5.2. *f*-models

For our *f*-models, we begin the simulations when the satellite has already reached the inner regions of the primary galaxy. A DSph galaxy on a low eccentricity orbit in these inner dense regions of the Galaxy undergoes stronger disruptions than on more eccentric orbits, because the tidal forces are stronger at all positions on the trajectory.

5.2.1. *f*-A satellite

In Fig. 2a (b), we plot the angular distribution of the *f*-A satellite along (perpendicular to) the orbit (which has eccentricity $e = 0.2$) as seen from 24 kpc away (it corresponds to the Solar neighbourhood viewpoint), for four snapshots. In this case, the lifetime of the dwarf galaxy, before significant disruption, is nearly 0.4 Gyrs (Fig. 3a).

The material from the satellite galaxy is tidally stripped, forming a long stream and then, after 1.2 Gyrs, an almost close great circle in an Aitoff projection, which survives for a long time (Fig. 4a). Moreover, as we can see in Fig. 2b, the mean width perpendicular to the orbit on the sky is 7° (it was only 1.9° at the initial time) and the projected surface brightness (Fig. 5a) is 5 mag fainter at the end of the simulation (after 2.1 Gyrs).

5.2.2. *f*-B1 and *f*-B2 satellites

For both *f*-B1 and *f*-B2 orbits ($e = 0.64$ and 0.75 , respectively), disruption mainly occurs at perigalacticon, because tidal forces are more efficient at small galactocentric radii. The lifetime of a satellite depends strongly on the orbit shape. The *f*-B1 satellite is destroyed after 0.5 Gyr (Fig. 3b) whereas the *f*-B2 satellite survives for 1 Gyr (Fig. 3c) due to the longer period of its orbit, at this time the *f*-B2 satellite undergoes a close *interaction* ($r \sim 2$ kpc) with the center of the primary galaxy and it is tidally destroyed.

The final destruction of dwarf galaxies is more efficient in our more eccentric orbits and they present fainter surface brightness at the end of the simulation than the satellite on a low eccentric orbit (Fig. 5). The satellite particles of *f*-B models are spread over all directions and no predominant streams are formed, as it can be seen in Fig. 4b for the *f*-B1 model. In Figs. 2d and 2f, we have represented the width (perpendicular to the orbit) of the stream. At the end of the simulations, the *f*-B2 models do not have any predominant peak in the mass distribution perpendicularly to the initial orbit.

As a general result, due to the tidal field on the satellite we observe: i) a modification of the internal structure of the satel-

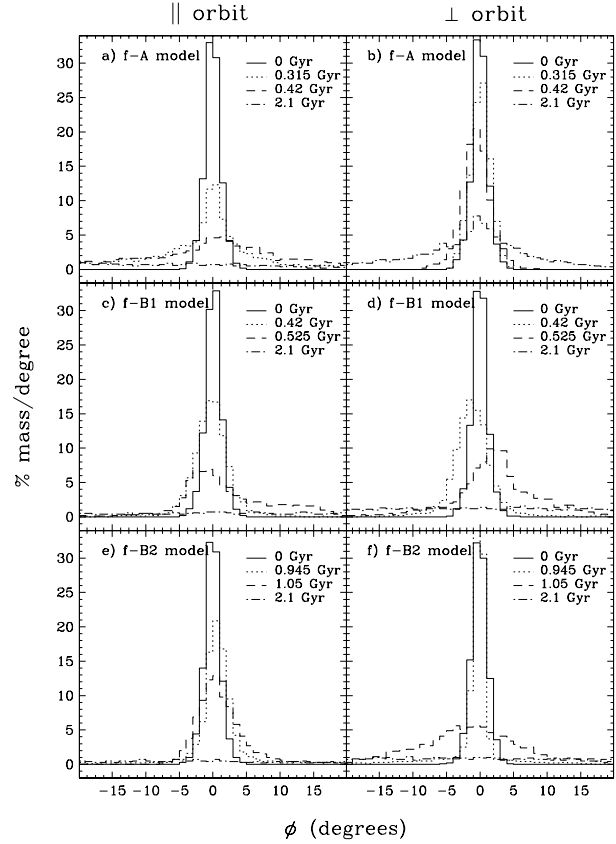


Fig. 2. *f*-models: mass distribution parallel (**a**, **c** and **e**) and perpendicular (**b**, **d** and **f**) to the orbit as function of the angle ϕ to the satellite center, as seen from 24 kpc away, which is the present distance between the Sun and the Sagittarius DSph

lite for both cases of orbits (eccentric and quasi-circular), with increase of the projected velocity dispersion, and ii) a continuous loss of satellite mass and luminosity. Anyone tempted to infer a $(M/L)_o$ ratio from such experiments by assuming virial conditions would find values 100 – 200 times higher than the true ones at the disruption time (Fig. 6), confirming the results of K97.

5.3. *s*-models

In this subsection, we analyze the interaction effects on a DSph in equilibrium with the galaxy potential. Either it could have fallen down slowly from an intermediate region in the denser parts of the primary galaxy, losing part of its mass and becoming a low DM satellite, or it could have been formed in a tidal tail of a major accretion event.

5.3.1. *s*-A model

DSphs which are theoretical equilibrium solutions to Sgr at a circular inner orbit are small and low mass galaxies. The tidal field is almost constant along this quasi-circular orbit and, therefore, interaction effects on the satellites in equilibrium are not important. For the *s*-A orbit, there is a continuous loss of

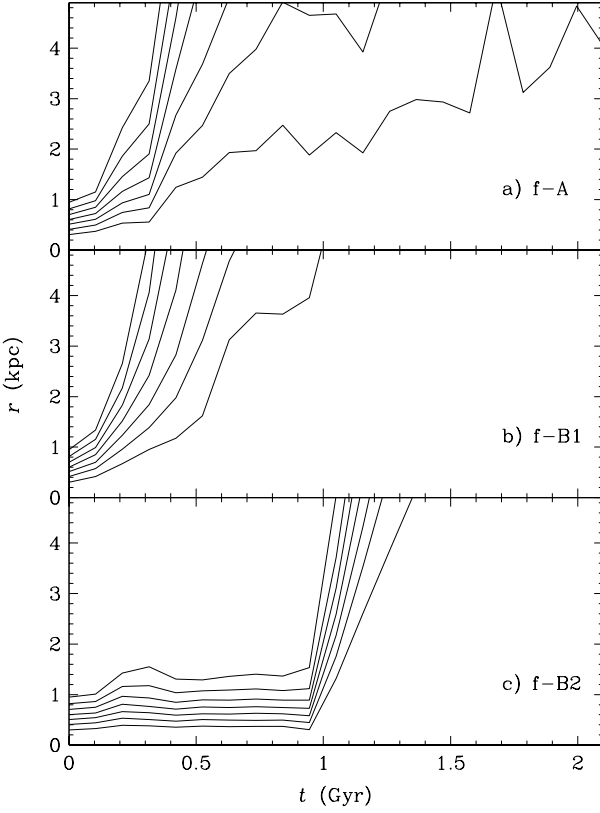


Fig. 3. Radii which enclose 70%, 60%, 50%, 40%, 30%, 20% and 10% of the initial mass of the satellite, for f-models

mass, but the satellite has still $\sim 20\%$ of the initial mass (Fig. 7c) after 2 Gyrs and it is still detectable (Fig. 7a). The central surface brightness has only changed by 2.5 mag (Fig. 7a), evolving from $21.3 \text{ mag arcsec}^{-2}$ to $24.8 \text{ mag arcsec}^{-2}$. The line-of-sight velocity dispersion grows in the outer parts of the satellite in agreement with findings by K97, remaining almost constant in average in the inner parts ($< 0.2 - 0.3 \text{ kpc}$) (Fig. 7b). We have calculated the mass inferred from the line-of-sight velocity dispersion, measured inside a radius of 0.5 kpc from the satellite center, using Eq. (1). Since the central velocity dispersion and the projected density (Fig. 7a) evolve slowly in the central region of the satellite at the beginning of the simulation, the inferred mass-to-luminosity ratio remains almost constant, contrary to the f-models. However, as we have explained above, the real mass of the satellite decreases and it is only $\sim 20\%$ of the initial value after 2 Gyrs. The structural evolution is slow (Fig. 7c) and it leads to a lower central surface brightness at the end of the simulation and a $(M/L)_o$ ratio calculated from the velocity dispersion (inside 0.5 kpc) which is 5 times higher than the real one (Fig. 7d). This effect could be dramatically increased if the velocity dispersion is measured inside a larger radius, because of the velocity dispersion increase in the outer region of the satellite, leading to a calculated $(M/L)_o$ ratio up to 10 times larger than the real one. Very faint tidal streams are formed, which are spread along $\sim 75 - 100\%$ of the orbit with a spatial width $\sim 6^\circ$ (Fig. 8).

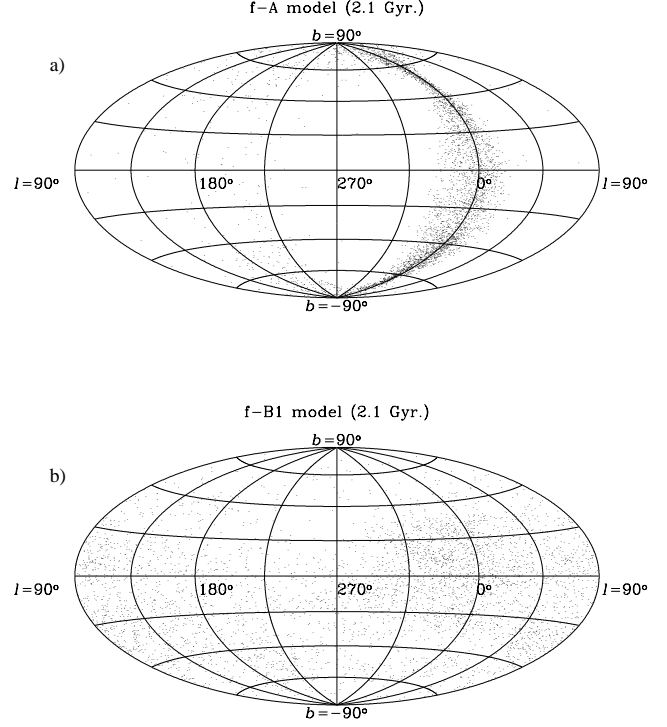


Fig. 4. Aitoff projection of the f-A and f-B1 models at the end of the simulation (2.1 Gyr)

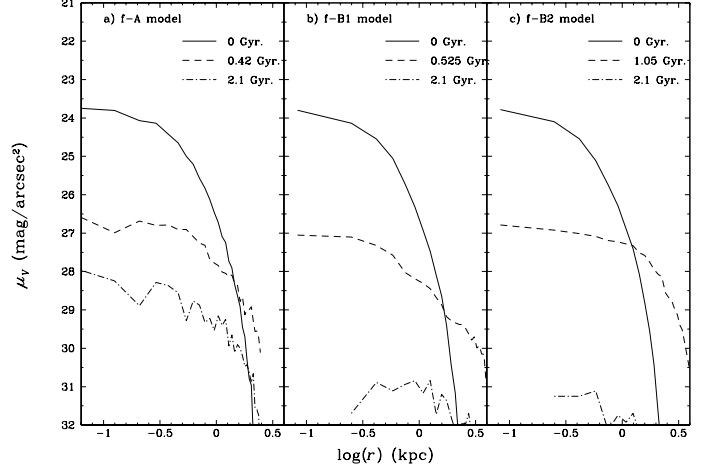


Fig. 5. Surface brightness μ_V of the f-models, assuming $(M/L)_{\text{real},V} = 10 M_\odot/L_\odot$

5.3.2. s-B models

Perigalacticon and apogalacticon of high eccentric s-B1 and s-B2 orbits decrease with the time. The most dramatic example is the **s-B1 orbit**. The DSph passes 1 kpc from the galaxy center at its third passage at perigalacticon (Fig. 9c), because of the orbital energy loss. During this passage the satellite is

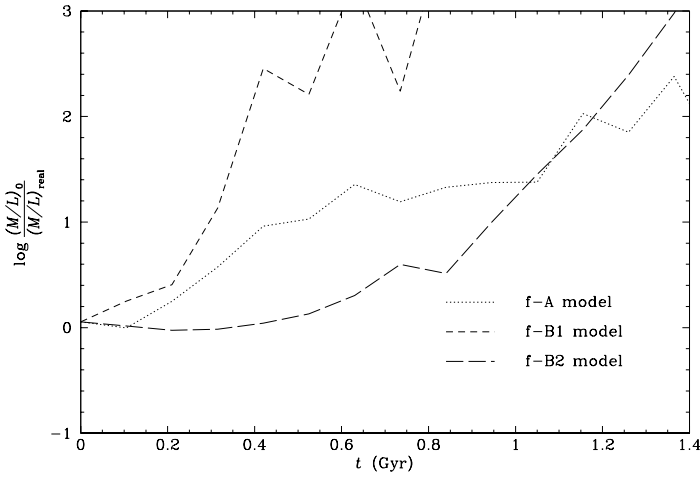


Fig. 6. Evolution of the log of the ratio between the mass-to-luminosity relation, $(M/L)_o$, inferred from the velocity dispersion values under dynamical equilibrium conditions, and the real mass-to-luminosity relation, $(M/L)_{\text{real}}$, for the f-models

strongly tidally stripped and it loses most of its mass (Fig. 9d). The surface brightness of the satellite decreases with time (Fig. 9a) and the velocity dispersion and the mass-to-luminosity ratio increase in the outer parts (Figs. 9b and 9e). The satellite is finally completely destroyed after nearly 1 Gyr.

s-B2 is the most external and eccentric orbit which we have chosen. As the other models, it fulfills at certain times the position and velocity constraints for the Sagittarius DSph orbit in the observational range (Ibata et al. 1997).

In order to investigate this case in more details, we have selected three different satellite models for orbiting on this trajectory (s-B2a, s-B2b and s-B2c). The concentration (defined as $c = \log(r_t/r_o)$) varies from 1.28 (s-B2a) to 0.83 (s-B2c). The concentration determines the fate of the satellite, as well as the evolution of the $(M/L)_o$ ratio. The more concentrated the satellite is, the less variation of the inferred $(M/L)_o$ ratio it suffers (Fig. 10).

The $(M/L)_o$ ratio in Fig. 10 has been calculated for the central region of the satellite (< 0.5 kpc), where the tidal effects on the mass and the velocity dispersion are weaker. However, even in the most concentrated satellite (s-B2a), we obtain $(M/L)_o$ ratios which are $\sim 10(M/L)_{\text{real}}$, these values rise up to several hundreds for the least concentrated model (s-B2c).

It is interesting to notice the strong variations of the inferred $(M/L)_o$ ratio with time. This behaviour is caused by the evolution of the surface mass density when the satellite suffers a close encounter with the core of the primary galaxy. It leads to a successive rearrangement of the internal structure of the satellite. Another important parameter in the $(M/L)_o$ calculations is the angle between the observer-satellite line and the main axis of the satellite. The strong anisotropies of the satellite (tails along the orbit, anisotropic velocity dispersion, etc) could

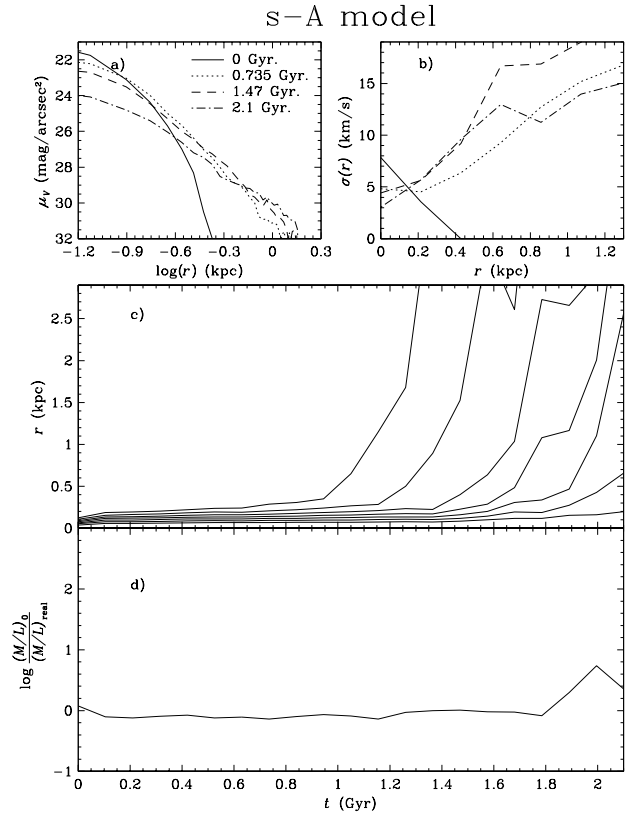


Fig. 7. s-A model: **a** surface brightness μ_V assuming $(M/L)_{\text{real},V} = 2 M_{\odot}/L_{\odot}$, **b** velocity dispersion of the satellite as a function of the radius as same timesteps as in a), **c** evolution of the radii which enclose from 70 to 10 % of mass of the satellite from the top to the bottom, and **d** evolution of the mass-to-luminosity ratio measured from the velocity dispersion. The observational values of μ , σ are given in Table 1

produce various $(M/L)_o$ values (as already suggested by K97 and KK98).

The line-of-sight velocity dispersion evolves as shown in Fig. 11. The projected velocity dispersion decreases in the central part of the satellite ($r < 0.5$ kpc) and it increases for $r > 0.5$ kpc. Thus, the $(M/L)_o$ ratio calculated from Eq. (1) varies, depending on the limit radius used for the measurement of the *central* velocity dispersion (this limit radius is related to the observational resolution).

s-B2a model:

The **s-B2a model** undergoes a long term evolution. It is the most concentrated model that we have chosen and it survives for at least 10 Gyrs. A mild loss of mass is produced, mainly at perigalacticon: the satellite loses the outer layers of mass, but a core enclosing 30% of the initial mass subsists (Fig. 12a). The limit radius is smaller than the initial one, but the half-brightness radius increases (the final satellite is less concentrated). The central surface brightness decreases (Fig. 13a),

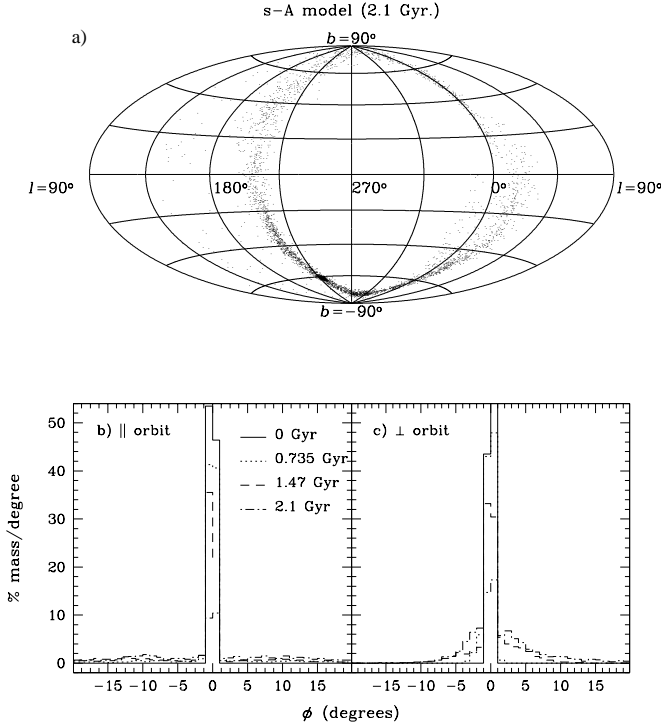


Fig. 8. **a** Aitoff projection of the s-A model at the end of the simulation (2.1 Gyr), and mass distribution **b** parallel and **c** perpendicular to the orbit as function of the angle ϕ to the satellite center

changing from ~ 21.0 mag arcsec 2 to ~ 22.0 mag arcsec 2 (assuming $(M/L)_{\text{real}} = 2 M_{\odot}/L_{\odot}$). The final s-B2a satellite is smaller ($r_{hb} = 0.13$ kpc) than the observed Sgr DSph ($r_{hb} = 0.55$ kpc) and the $(M/L)_o$ ratio is not large enough to reproduce the inferred $(M/L)_o = 50 M_{\odot}/L_{\odot}$ by Ibata et al. (1997).

s-B2b model:

The mass loss of the **s-B2b satellite** (Fig. 12b) is stronger than that of the s-B2a satellite. The particles of the satellite outer region are stripped, mainly at perigalacticon. The tidal stripped material develops a stream forward and backward from the satellite along the orbit. In Fig. 13b, a low surface brightness tidal extension of the satellite can be seen at intermediate epochs. At the final snapshot ($t = 10.5$ Gyr), the residual core of the satellite is still detectable, it has $\sim 15\%$ of the initial mass (Fig. 12b) and a central projected surface brightness $\mu_o \sim 23.8$ mag arcsec $^{-2}$ assuming $(M/L)_{\text{real}} = 2 M_{\odot}/L_{\odot}$. The initial central surface brightness for the same $(M/L)_{\text{real}}$ ratio was 21.3 mag arcsec $^{-2}$. The stream formed close to the satellite has a surface brightness which is 5.0-6.5 mag fainter than the center of the satellite. This stream is similar to those formed by extra-tidal stars observed close to some DSph satellites.

At some snapshots (i.e. 3.7 Gyr, 4.83 Gyr, 6.2 Gyr, 7.3 Gyr, 8.45 Gyr and 9.6 Gyr), when the tidal streams of the satellite

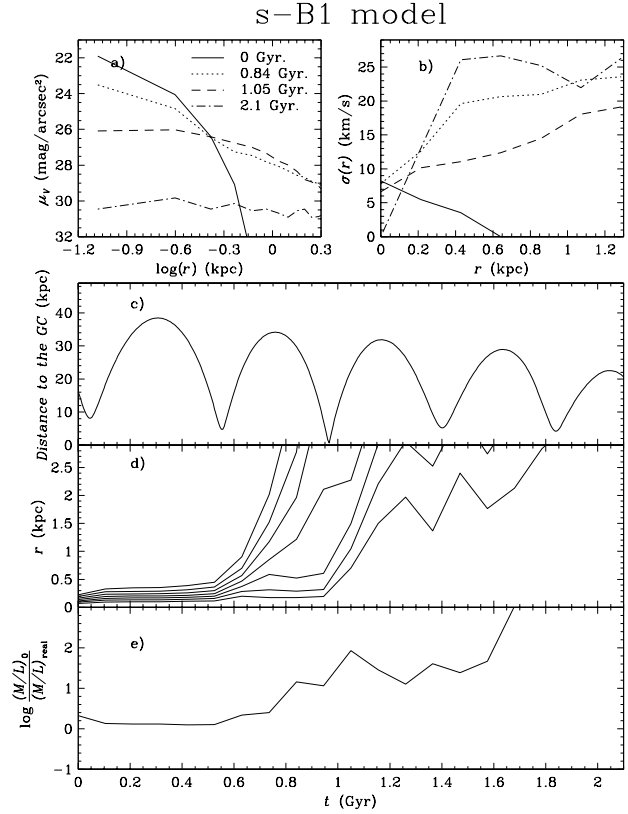


Fig. 9. s-B1 model: **a** surface brightness μ_V assuming $(M/L)_{\text{real},V} = 2 M_{\odot}/L_{\odot}$, **b** velocity dispersion of the satellite as a function of the radius, **c** distance to the satellite the Galactic Center, **d** evolution of the radii which enclose 70, 60, ..., 10% of the satellite mass (lines from left to right), and **e** evolution of the mass-to-luminosity ratio measured from the velocity dispersion. The observational values of μ and σ are given in Table 1

are already formed, the radial velocity, v_r , and the gradient of the radial velocity, $|dv/db|$, of the s-B2b satellite and of the stream around the satellite reproduce the observations of Sgr DSph region. The observational values of v_r and $|dv/db|$ of Sgr are given in Table 1. However, the values of both quantities in the models are strongly dependent on the position and orientation of the orbit. Therefore, small perturbations in the orbit of the models could lead to differences in v_r of several 10 km s $^{-1}$. In general, the sign of the variation of the radial velocity depends on the position of the satellite along the orbit. For some particular positions, the radial velocity gradient is almost 0 km s $^{-1}$ /degree. The s-B2b satellite at time 8.47 Gyr is an example of a model which has a good agreement in position with the observations of Sgr DSph (Fig. 14c). From the kinematical point of view, the particles in the stream show a velocity gradient $|dv/db| \sim 4$ km s $^{-1}$ /degree (Fig. 14a), which is slightly higher than the observed value ($|dv/db| = 3$ km s $^{-1}$ /degree), whereas the radial velocity is slightly lower. Moreover, this

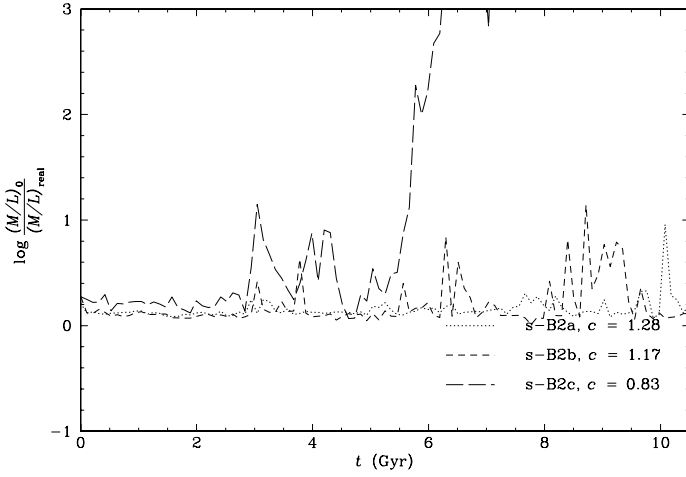


Fig. 10. Evolution of the log of the ratio between the mass-to-luminosity relation, $(M/L)_o$, inferred from the velocity dispersion values, and the real mass-to-luminosity relation, $(M/L)_{\text{real}}$, for s-B2 satellites. The parameter $c = \log(r_t/r_o)$ is the concentration of the model

satellite model presents a velocity dispersion ($\sigma \sim 6$ km/s, Fig. 14b) lower than the observed value ($\sigma \sim 11.4$ km/s). However, the projected velocity dispersion of the stream remains almost constant and equal to the velocity dispersion in the inner region of the system. Observational data show that regions close to the Sagittarius globular clusters (Terzan 8, Terzan 7, Arp 2) have a similar projected velocity dispersion (Ibata et al. 1997).

The density contour map of the s-B2b model at 8.47 Gyr (Fig. 14c) resembles the observational map for the region around the center of the satellite (see for example Fig. 1 in Ibata et al. 1997), in spite of the low resolution (few mass points) of the simulation. However, the center of our satellite has a steeper density profile, the half-brightness radius of the model is $r_{hb} = 0.12$ kpc and that of Sagittarius DSph is 0.55 kpc. Even at the end of the simulation ($t = 10.5$ Gyr) the satellite remains too concentrated ($r_{hb} = 0.17$ kpc). This discrepancy could mean that either the real Sagittarius DSph has undergone a stronger tidal field, which has caused an effective destruction of the satellite core, or it has suffered tidal disruption for a longer time, or the initial density profile of the Sagittarius satellite was more extended than that of our model. In order to test the latter hypothesis, we have built the s-B2c model, which is less concentrated than s-B2b but more massive. s-B2c follows the same orbit as s-B2b.

s-B2c model:

The **s-B2c satellite** survives 5.5 Gyr before disruption. The effects at perigalacticon (Fig. 12c) are stronger than those of the other s-B2 models, because of the lower concentration. Low surface brightness trailing and leading streams are formed. At 5.88 Gyr, the residual satellite looks like a long tidal extension with a maximum projected surface brightness $\mu \sim 27.0$ mag arcsec $^{-2}$, assuming $(M/L)_{\text{real}} = 2 M_{\odot}/L_{\odot}$ (Fig. 13c).

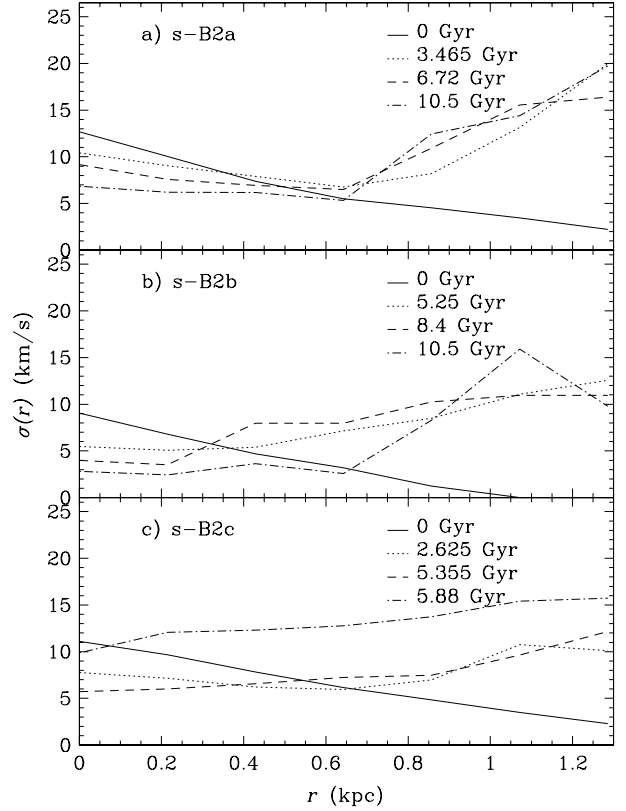


Fig. 11. Velocity dispersion, $\sigma(r)$, at four snapshots, for s-B2 satellites

The line-of-sight velocity dispersion evolves as shown in Fig. 11c. In the outer region of the satellite it increases up to an almost constant velocity dispersion along the orbit. At the last snapshot of Fig. 11c (5.88 Gyr) the satellite is already disrupted and the velocity dispersion of the remnant stream has increased with respect to the value before destruction.

The central $(M/L)_o$ ratio obtained from Eq. (1) depends on the position of the satellite along the orbit (Fig. 10). The most important variations in the $(M/L)_o$ ratio are observed at the perigalactic passage. At this time the satellite is compressed and stretched, its internal distribution is modified and the tidal extensions are more pronounced. At the final steps of the evolution, the more stripped the satellite is, the higher measured the $(M/L)_o$ is.

We have analyzed the satellite characteristics at 5.38 Gyr from the beginning of the simulation. It corresponds to the last approach to the galactic disc and after the last perigalacticon, which produces total disruption. At this time, the position ($b = -10.7^\circ$) and the Galactic velocity ($(U, V, W) \sim (214, 0, 170)$ km s $^{-1}$) of the satellite agree with the observational data. In Fig. 15, the kinematical distribution (radial velocity and line-of-sight velocity dispersion) along the orbit and the contour density maps are shown. The half-brightness radius, r_{hb} , and central surface brightness, μ_o , of the model roughly fit the observations (Table 1). The values we obtain in the s-B2c simulation at 5.38 Gyr are $r_{hb} \sim 0.4$ kpc and $\mu_o \sim 24.3$ mag

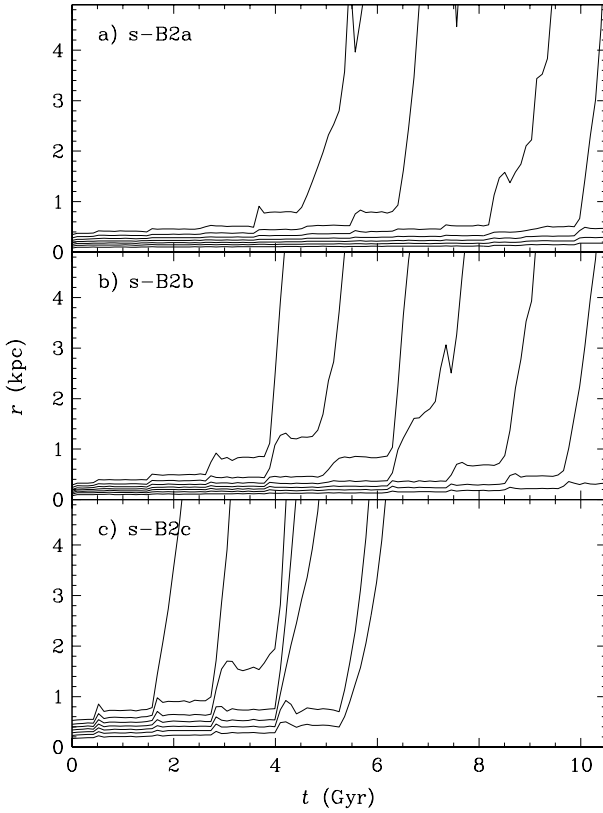


Fig. 12. Radii which enclose 70%, 60%, 50%, 40%, 30%, 20% and 10% of the initial mass of the satellite, for s-B2 models

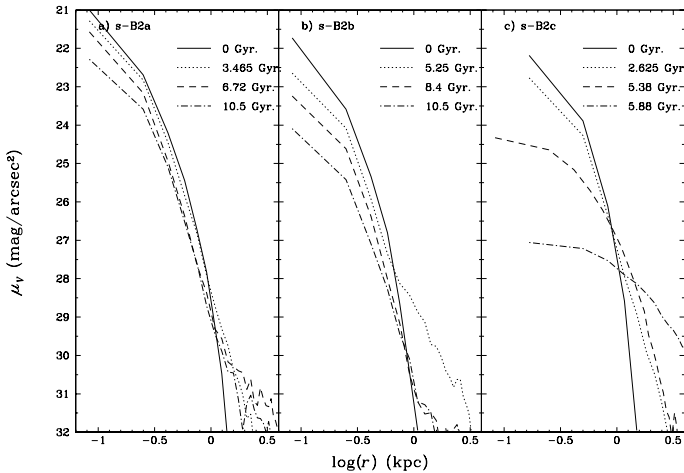


Fig. 13. Surface brightness μ_V of the s-B2 satellites, assuming $(M/L)_{\text{real},V} = 2 M_{\odot}/L_{\odot}$

arcsec^{-2} , which are slightly lower than observational values, but they evolve to larger half-brightness radius and lower surface brightness as the satellite approaches the Galactic disc and gets more disrupted. For example, at $t = 5.565$ Gyr we obtain the best accord between the simulations and the ob-

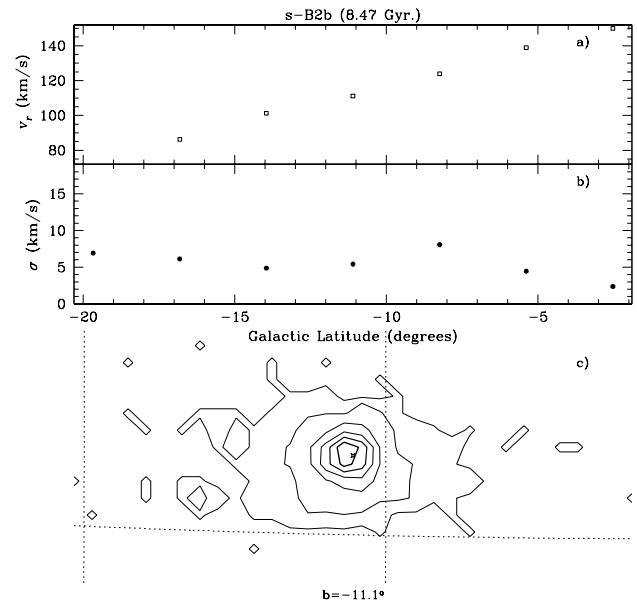


Fig. 14. s-B2b satellite, at 8.47 Gyr: **a** Radial velocity, v_r , along the orbit (constant galactic latitude), **b** velocity dispersion, σ , along the orbit and **c** contour density map at the same scale as the a) and b) plots (the star represents the mass center of the satellite, located at $b = -11.1^\circ$), the contours correspond to $\mu = 23.2, 23.6, 24.0, 24.7, 26.8$ and 28.7 mag arcsec^{-2} from the center

servations for r_{hb} and μ_o (the values of the model are 0.5 kpc and $25.4 \text{ mag arcsec}^{-2}$, respectively), but the position and the velocity do not reproduce the observations ($b \sim 20^\circ$ and $(U, V, W) \sim (103, 0, 86) \text{ km/s}$).

The radial velocity gradient along the orbit of s-B2c satellite depends on the orientation of the trajectory, as in the s-B2b model. At 5.38 Gyr we obtain $|dv/db| \sim 1.5 \text{ km s}^{-1}/\text{degree}$ for the trailing stream, which is lower than the observed value. However, the radial velocity v_r is in agreement with the observations ($v_r = 171 \text{ km s}^{-1}$). The satellite velocity dispersion measured inside 0.5 kpc has decreased ($\sigma \sim 7 \text{ km/s}$), but it is still large enough to give $(M/L)_o \sim 10(M/L)_{\text{real}}$.

It is interesting to analyze not only the region around the center of mass of the satellite but also the tidal tails which are formed along the orbit. We have done it for several tidal tails close to the satellite. In Fig. 16, we plot the surface brightness of the trailing tail of the s-B2c model at various timesteps, assuming $(M/L)_{\text{real}} = 2 M_{\odot}/L_{\odot}$ (a larger value of $(M/L)_{\text{real}}$ moves the lines down in the figure and vice versa). The simulations are compared with the trailing tail observed by Mateo et al. (1998) recently. As we can see, except for the region closest to the satellite center ($< 12^\circ$), the simulations reproduce the observations, giving a better result when the satellite is more disrupted. This supports the hypothesis that Sgr DSph is close to its destruction. In our simulations, we also obtain a leading tail similar to the trailing one. Unfortunately,

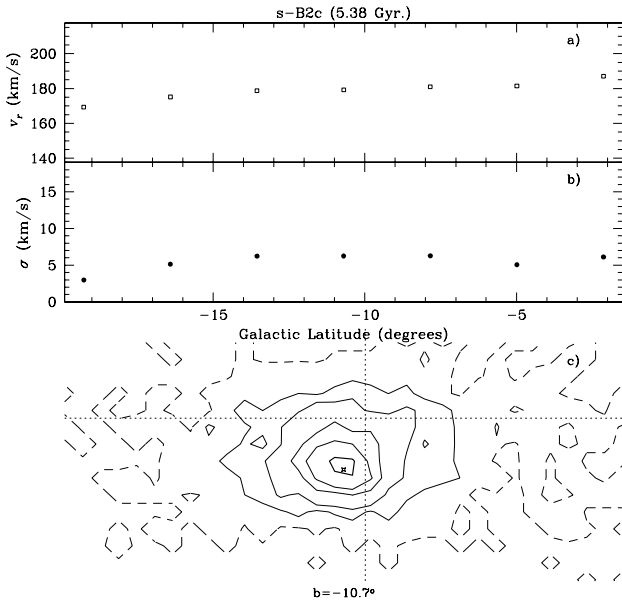


Fig. 15. s-B2c satellite, at 5.38 Gyr: **a** Radial velocity, v_r , along the orbit (constant galactic latitude), **b** velocity dispersion, σ , along the orbit and **c** contour density map (the star represents the mass center of the satellite, located at $b = -10.7^\circ$), the solid contours correspond to $\mu = 24.3, 25.0, 25.5, 26.7, 27.5$ mag arcsec $^{-2}$ from the center and the dashed contour corresponds to $\mu = 30$ mag arcsec $^{-2}$

the proximity of the Galactic disc to Sgr center makes difficult to test this result of symmetric tails due to still poor observational data. To give another example of the complexity of the satellite structure, we plot in Fig. 17 the contour density levels and the kinematic behaviour of a tidal tail, at 5.25 Gyrs from the beginning of the simulation. It looks like the Sgr DSph from the kinematical point of view, having radial velocity (Fig. 17a) and velocity dispersion (Fig. 17b) similar to Sagittarius observed values ($v_r = 171$ km s $^{-1}$ and $\sigma = 11.4$ km s $^{-1}$). The shape of the tail (Fig. 17c) also looks like a tidally disrupted satellite, however, the central surface brightness is $\mu_o \sim 29.5$ mag arcsec $^{-2}$ (fainter than a typical DSph) and the computed $(M/L)_o$ ratio is $200(M/L)_{\text{real}}$ (higher than the estimation for DSph galaxies). Nevertheless, this example illustrates, on one hand, the difficulty of distinguishing between a tidal tails and a DSph galaxy when the latter is close to the disruption and, on the other hand, the possibility of identifying objects (globular clusters, etc) which have been tidally disrupted from a satellite galaxy by measuring their kinematic characteristics.

6. Discussion

Summing up the results obtained in our simulations and comparing them with other published works, we agree with other authors (Velázquez & White 1995; Ibata & Lewis 1998) that Sgr DSph has a short period orbit ($T \leq 1$ Gyr). This constraint

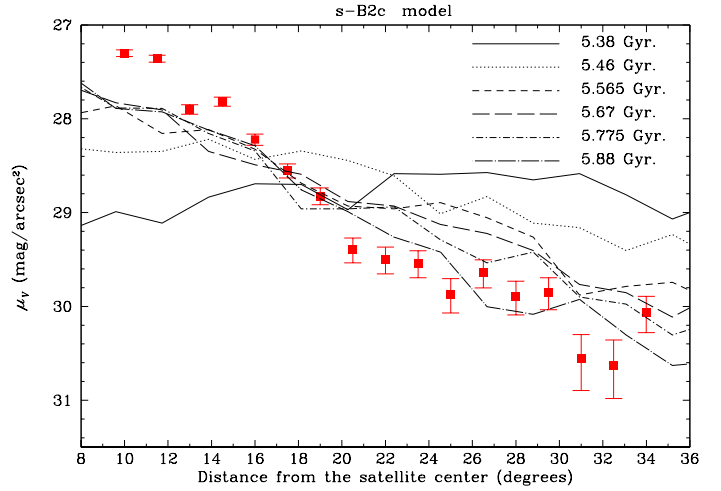


Fig. 16. Surface brightness μ_V of the tidal tail close to the Sgr satellite. Lines represent the s-B2c model at various timesteps. Filled squares are the data (with the errorbars) by Mateo et al. (1998)

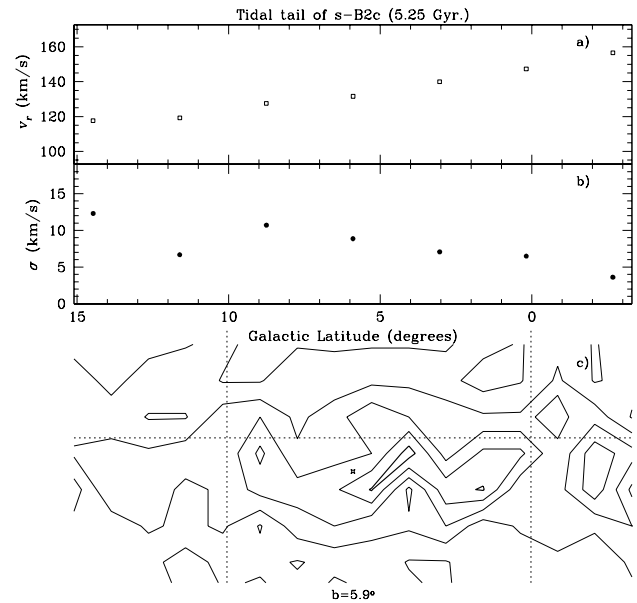


Fig. 17. Tidal tail of the s-B2c satellite: **a** Radial velocity, v_r , along the orbit (constant galactic latitude), **b** velocity dispersion, σ , along the orbit and **c** contour density map (the star represents the mass center of the satellite, located at $b = 5.9^\circ$) and the contours correspond to $\mu = 29.6, 29.9, 30.3, 30.8, 32.0$ mag arcsec $^{-2}$

comes from measurement of the position and the radial velocity of Sgr DSph in a realistic model of the Galaxy. However, we disagree about the DM content. These previous works claim that Sgr DSph is a DM dominated satellite, because, contrary to us, they could not obtain a low mass satellite which survives

by orbiting in the potential of the Galaxy. Therefore, they cannot explain the complex evolutionary pattern inferred for the Sagittarius DSph, which has suffered a chemical enrichment and evolution and the age interval of its globular clusters which suggests a long life orbiting in the Galaxy.

Ibata & Lewis (1998) have tested low massive models in order to reproduce the Sgr DSph characteristics, reaching an unsuccessful result on the matter and concluding that Sgr DSph must have a large DM content. There are two differences between their study and ours. Firstly, they use a rigid potential to model the Galaxy, so no energy interchange is allowed between the satellite and the Galaxy. This restriction could eventually prevent a readjusting of the internal energy of the satellite in order to reach an equilibrium with the environment. Even if the energy transfer from the satellite to the halo is not important in all cases, we emphasize that our treatment is *a priori* adaptable to satellites of various masses. Secondly (and mainly), Ibata & Lewis (1998) do not take into account the tidal potential of the Galaxy as they build their satellite model. We have confirmed that the fate of such satellites is different from that of the satellites in equilibrium with the tidal potential as considered here. Consequently, a more accurate model of the initial satellite, that reflects the true dynamical situation of the DSph, is required in order to avoid spurious effects in the simulations. These differences in the models are responsible for the opposite conclusions reached by Ibata & Lewis, compared with ours concerning DM. Furthermore, the recent observations of Sgr by Mateo et al. (1998) prove the existence of a long trailing tail, which supports the hypothesis that Sgr DSph has suffered strong tidal forces, it is close to disruption and, therefore, it is not in virial equilibrium. The existence of this tail also reduces the inferred $(M/L)_o$ ratio.

Our low DM satellites (*modified King's models*) establish important restrictions on the satellite formation theory. Thus, the satellite galaxies grow either in a quasi-isolated region (falling slowly on the center of the primary galaxy and having time for readjusting their internal structure to the tidal forces), or inside the main galaxy, in the tidal tails of a major accretion event, which automatically implies equilibrium with the tidal forces at the satellite formation epoch. Furthermore, the survival time of the *equilibrium* satellites in the potential of the Galaxy depend on the initial concentration of the DSph (the larger concentration, the longer the life-time). We have obtained models (i.e., s-B2a) which survive more than 10 Gyr. The evolution of these satellites gives rise to tidal streams and modifications on the outer velocity dispersion of the satellite and it leads to high observed mass-to-light ratios if dynamical equilibrium is assumed. We have obtained a rather good qualitative agreement with the observational constraints for the model s-B2c in a time interval (from 5.38 to 5.7 Gyr), although this agreement is not achieved simultaneously on all the constraints. We remind that the simulation time does not necessarily correspond with the age of the oldest globular cluster of Sgr and, therefore, the s-B2c model is not necessarily in disagreement with the observations. In this case, two possibilities could be invoked to explain the age of the oldest Sgr globular clusters:

(i) either the satellite has been orbiting for a long time in a more external region (where tidal forces are smaller), it suffers dynamical friction or/and a deflection with a dense structure of the MW and it reaches the present orbit where, eventually, it is disrupted, or (ii) it has formed in a tidal tail which contained an old stellar population (Kroupa 1998c).

The tidal tail models illustrate that a DSph without DM orbiting through central regions of the Galactic potential could preserve its structural parameters for a long time. Later on, the DSph could show high inferred $(M/L)_o$ values as it becomes disrupted. The only restriction of the model is that the satellite must reach the central regions of the Galaxy in equilibrium with the tidal forces. That could be possible whether the satellite has been formed in a tidal tail of an accretion event or it has been slowly accreted from the external parts of the Galaxy. The latter possibility could increase the estimated life-time of the satellite before destruction.

Recently, K98 has discussed the parameter space of the DSphs which could survive in a tidal field. In spite of the different initial distribution functions, our s-models seem to be located in the available region of the (M_{sat}, r_{sat}) space for surviving satellites. However, the main difference between the approaches to the problem is that we build the model of the satellite initially in equilibrium with the tidal forces by solving the Boltzmann equation (Gómez-Flechoso & Domínguez-Tenreiro 1998) and that assures *a priori* the survival of the satellite for a long time.

7. Summary

We have performed simulations of Sagittarius-like satellites to follow the evolution of these systems. The satellite and the primary galaxy are modelled as N-body systems, that prevents possible purely numerical effects which could appear in a non-selfgravitating scheme (i.e. if one of the interacting system is represented by a rigid potential). Two satellite models have been tested:

1. First of all, we have used *isolated King's models* (three free parameter models) for the satellite, but they are tidally stripped and destroyed in a short interval of time, undergoing a fast evolution.
2. In order to correctly model the observed situation we had to introduce the *modified King's models* (two free parameters-models), which allow us to build up the distribution function of the satellite, taking into account the tidal force of the environment. These s-models could correspond to no DM dominated satellites. In this framework, the initial concentration of the satellite and the trajectory determine its life-time. Central circular orbits lead to more effective tidal destruction events than highly eccentric orbits. For a given kind of orbit, the most concentrated satellites live longer. The model which better reproduces the observations is the s-B2c model after orbiting 5.38-5.6 Gyr in the potential of the Milky Way. For the same orbits, the s-models survive a longer time orbiting in the Galactic potential than

the f-models, despite the s-models having smaller masses (smaller binding energies).

According to the results presented here, our main conclusions about the evolution of Sgr are:

1. Sagittarius may not be a dominated DM satellite.
2. It follows an eccentric orbit (perigalacticon and apogalacticon are approximately 15 and 70 kpc).
3. It was more concentrated in the past than at the present epoch.
4. It could have been orbiting in the Galactic halo for a long time (minimum 5 Gyr).

As general conclusions about the DSph satellites, we can remark that:

1. High values of $(M/L)_o$ found in the literature (Ibata et al. 1995; Irwin & Hatzidimitriou 1995; Mateo 1998 for a review of the Galactic satellites) could be due to an erroneous use of the virial theorem and not to the presence of DM (as already suggested by K97; KK98).
2. The progenitor of these satellite could be either lumps formed in a major accretion event or other dwarf galaxies (maybe dwarf irregulars or dwarf spirals) which fall in the potential well of the Galaxy, lose their gas content and evolve to the equilibrium configuration in the tidal field of the Milky Way, giving rise to the population of DSphs. The finding of intermediate states of this evolution could be a support to the proposed scenario.
3. According to some of the present results, some DSphs are able to survive for long times orbiting in the Galactic halo. That should be taken into account for the calculations of the dissolution rate of dwarf galaxies in the halo of the primary galaxy.

Acknowledgements. We would like to thank D. Pfenniger and D. Friedli for critically reading the paper, as well as the referee for remarks which have led to clarify various points of the paper. M.A. Gómez-Flechoso was supported by the Fundación Ramón Areces through a fellowship. This work has been partially supported by the Swiss National Science Foundation.

References

- Alard, C., 1996, ApJ 458, L17
- Barnes J.E., Hernquist L., 1992, Nature 360, 715
- Barnes J.E., Hut P., 1986, Nature 324, 446
- Becklin E.E., Neugebauer G., 1968, ApJ 151, 145
- Burkert A., 1997, ApJ 474, L99
- Cole S., Aragón-Salamanca A., Frenk C.S., Navarro J.F., Zepf S.E., 1994, MNRAS 271, 781
- Duc P.A., Mirabel I.F., 1997. In: Sanders D.B. (ed.), IAU Symposium 186: Galaxy Interactions at Low and High Redshift, preprint astro-ph/9711253
- Edelsohn D.J., Elmegreen B.G., 1997, MNRAS 290, 7
- Fux R., 1997, A&A 327, 983
- Gómez-Flechoso M.A., Domínguez-Tenreiro R., 1998, MNRAS, submitted
- Ibata R.A., Lewis G.F., 1998, ApJ 500, 57
- Ibata R.A., Gilmore G., Irwin M.J., 1994, Nature 370, 194
- Ibata R.A., Gilmore G., Irwin M.J., 1995, MNRAS 277, 781
- Ibata R.A., Wyse F.G., Gilmore G., Irwin M.J., Suntzeff M.B., 1997, AJ 113, 634
- Irwin M., Hatzidimitriou D., 1995, MNRAS 277, 1354
- Johnston K.V., Spergel D.N., Hernquist L., 1995, ApJ 451, 598
- Johnston K.V., Hernquist L., Bolte M., 1996, ApJ 465, 278
- King I., 1966, AJ 71,64
- Klessen R.S., Kroupa P., 1998, ApJ 498, 143
- Kroupa P., 1997, New Astronomy 2, 139
- Kroupa P., 1998. In: Duschl W., Einzel C. (eds.) Dynamics of Galaxies and Galactic Nuclei, preprint astro-ph/9801047
- Kroupa P., 1998b. In: Richtler T., Braun J.M. (eds.) The Magellanic Clouds and Other Dwarf Galaxies, preprint astro-ph/9804255
- Kroupa P., 1998c, MNRAS 300, 200
- Layden A.C., Sarajedini A., 1997, ApJ 486, L107
- Lynden-Bell D., 1982, The Observatory 102, 202
- Lynden-Bell D., Lynden-Bell R.M., 1995, MNRAS 275, 429
- Mateo M., 1994. In: Meylan G., Prugniel P. (eds.) ESO/OHP Workshop on Dwarf Galaxies. ESO, Garching, p. 309
- Mateo M., 1997. In: Arnaboldi M., Da Costa G.S., Saha P.(eds.) The Nature of Elliptical Galaxies, in press
- Mateo M., Mirabal N., Udalski A., Szymański M., Kałużny J., Kubiak M., Krzemiński W., Stanek K. Z., 1996, ApJ 458, L13
- Mateo M., 1998, ARA&A 36, 435
- Mateo M., Olszewski E.W., Morrison H.L., 1998, preprint astro-ph/9810015
- Matsumoto T., Hayakawa S., Koizumi H. et al., 1982. In: Riegler G., Blandford R. (eds.) The Galactic Center. American Institute of Physics, New York, p. 48
- Merritt, D., 1996, AJ 111, 2462
- Montegriffo P., Bellazzini M., Ferraro F.R., Martins D., Sarajedini A., Fusi Pecci F., 1998, MNRAS 294, 315
- Oh K.S., Lin D.N.C., Aarseth S.J., 1995, ApJ 442, 142
- Piatek S., Pryor C., 1995, AJ 109, 1071
- Preston G.W., Shectman S.A., Beers T.C., 1991, ApJ 375, 121
- Richstone, D.O., Tremaine, S., 1986, AJ 92, 72
- Theis, Ch., Spurzem, R., 1999 A&A 341, 361
- Velázquez H., White S.D.M., 1995, MNRAS 275, L23
- Whitlock P.A., Irwin M., Catchpole R. M., 1996, New Astronomy 1, 57
- Zinn R., 1985, ApJ 293, 424